 ICCES, vol.15, no.4, pp.153-160

Anisotropic elastic properties of Ni-Mn-In magnetic shape memory alloy

K. Williams[1], **T. Cagin**[1,2]

Summary

Designing magnetic shape memory materials with practicable engineering applications requires a thorough understanding of their electronic, magnetic, and mechanical properties. Experimental and computational studies on such materials provide differing perspectives on the same problems, with theoretical approaches offering fundamental insight into complex experimental phenomena. Many recent computational approaches have focused on first-principles calculations, all of which have been successful in reproducing ground-state structures and properties such as lattice parameters, magnetic moments, electronic density of states, and phonon dispersion curves. With all of these successes, however, such methods fail to include the effects of finite temperatures, effects which are critical in understanding how these properties couple to the experimentally-observed martensitic transformation. To this end, we apply the quasi-harmonic theory of lattice dynamics to predict the finite-temperature mechanical properties of Ni-Mn-In magnetic shape memory alloy. We employ first-principles calculations in which we include vibrational contributions to the free energy. By constructing a free energy surface in volume/temperature space, we are able to evaluate key thermodynamic properties such as entropy, enthalpy, and specific heat. We further report the elastic constants for the austenite and martensite phases and evaluate their role as a driving force for martensitic transformation.

Keywords: Magnetism, Elasticity, Shape memory alloys, DFT, Active materials.

Introduction

Magnetic shape memory alloys (MSMAs) differ from traditional, thermally activated SMAs in that they are characterized by strong magnetoelastic coupling. The Heusler-type metals, such as Ni-Mn-X (X:Al,Ga,In,Sn,Sb), undergo martensitic transformations that are sensitive to alloy composition, external pressure, and applied magnetic field. Certain compositions display unique structural responses to external magnetic fields, undergoing either magnetic twin reorientation or field-induced phase transformations that lead to a macroscopic shape memory effect. In Ni-Mn-Ga, this effect generates recoverable strains that are an order-of-magnitude

[1]Materials Science and Engineering, Texas A&M University, college Station, TX, U.S.A.
[2]Chemical Engineering, Texas A&M University, College Station, TX, U.S.A.

larger than those associated with the most common commercial magnetostrictors[1] Since this discovery, Mn-based Heusler compounds have been heavily studied, both through experimental probing of structure-property relationships and theoretical modeling of the underlying mechanisms.

In the Ni-Mn-In system, martensitic transformation has only been observed for compositions with increased Mn content[2,3] This magnetic-field-induced transition is driven by the relative size of magnetization between the parent and martensite phases, with stabilization of the austenite at high fields[2] Alloys of Ni-Mn-In undergoing these transitions exhibit large magnetic-field-induced strains[2], giant (sometimes inverse) magnetocaloric effect[2,4–6], and high magnetoresistance[6–8], making them attractive materials for a myriad of engineering applications beyond merely shape memory devices. Commonly cited uses include actuation, sensing, energy harvesting, and magnetic refrigeration[4,5,7]

Some In-containing MSMAs undergo martensitic transformations in which the sign of the magnetic exchange interaction flips, a so-called "metamagnetostructural" transition. Such a transition is sensitive to and can be driven by application of an external magnetic field. The result is low-temperature kinetic arrest of the martensitic transformation at high fields[9,10]

These physical behaviors indicate the presence of strong magneto-structural coupling in the Ni-Mn-In system. Magnetic ordering is known to be a function of Mn-Mn distance—with spins interacting via the RKKY exchange[11]—and more recent investigations have shown that structural transitions can be controlled by an effective "magnetic response" of the lattice to external fields. The latter is sensitive to temperature, and, while some understanding of structure and magnetic ordering has been obtained through first-principles studies[12], a fundamental constraint of traditional *ab initio* methods is the inability to include temperature effects.

For example, phonon calculations of the $L2_1$austenite structure of Ni_2MnIn show imaginary frequencies in the lowest acoustic mode. This indicates that vibrational instability exists at 0 Kelvin but says nothing about lattice stability at elevated temperatures[13] In a first attempt to include thermal effects, Enkovaara *et. al.* calculated the free energy of both the austenite and martensite phases of Ni_2MnGa by including vibrational energies determined from the Debye model. The martensitic phase transformation was successfully captured, with a theoretical transition temperature close to the experimental value[14] In a more recent work, Uijttewaal, *et. al.* have also considered the modulated premartensitic structure of Ni_2MnGa. By including quasi-harmonic phonons and fixed-spin-moment magnons, they have been able to reproduce the full sequence of phase transitions (austenite→premartensite→martensite) as a function of temperature[15] To our knowledge, this is the first instance of using first-principles methods to directly predict martensitic transformation and finite-

temperature phase stability in any Mn-based MSMA.

In this work, therefore, we employ the quasi-harmonic theory of lattice dynamics to calculate the free energy of the austenite and martensite phases of stoichiometric Ni_2MnIn. We compare the relative energies in order to discuss phase stability, predicting whether martensitic transformation will occur at this alloy composition. We also report thermodynamic properties such as entropy, enthalpy, and specific heat. We further calculate the elastic constants for the austenite and martensite phases and evaluate their role as a driving force for martensitic transformation.

Theory

We calculate ground-state total energies and phonon spectra for the $L2_1$ austenite and non-modulated $L1_0$ martensite of Ni_2MnIn using the Vienna ab initio simulation package (VASP)[16] and the implemented projector augmented wave (PAW) pseudopotential formalism[17] The electronic exchange and correlation functions are treated within Density Functional Theory using the generalized gradient approximation (GGA)[18].

For the austenite phase, we use a cubic unit cell with lattice parameter $a = 6.07$. The martensite is taken to be a tetragonal cell with $c/a = \sqrt{2} \approx 1.41$. All calculations are spin-polarized with an energy cut-off of 400 eV and an $8\times8\times8$ $k-$point mesh for Brillouin-zone integrations ($12\times12\times8$ for the tetragonal cell). Phonon dispersions are calculated for each phase by diagonalization of the corresponding dynamical matrix. Composed of all pairwise interatomic forces, this matrix is calculated for each linearly independent atomic displacement in a $2\times2\times2$ supercell of the relaxed, ground-state structure. The tetragonal supercell results in six such displacements, while the cubic only requires three.

Free energies for each phase are calculated by extension of the harmonic approximation to several points on the potential energy curve. These points, or quasi-harmonic steps, are represented by scaling the volume of the ground-state structure so as to simulate thermal expansion with temperature. To generate the free energy surface, we consider a total of five quasi-harmonic steps: the equilibrium volume, V_0 (determined from relaxation of the unit cell), and four volume expansions, $V_0 \pm 1\%$ and $V_0 \pm 2\%$. The free energy at each quasi-harmonic step is given by

$$F(V,T) = E(V) + F_{\text{vib}}(V,T), \tag{1}$$

where $E(V)$ is the energy of the motionless lattice, and $F_{vib}(V,T)$ is the vibrational energy of the harmonic system, both at the fixed volume V. We have neglected other thermally-excited degrees of freedom, i.e. the electronic and anharmonic

corrections to the free energy. Magnetic contributions are not treated explicitly, either. Rather, magnetization is allowed to vary with volume.

The vibrational term for a given volume is found by integrating over the phonon density of states, $g(\upsilon)$, according to the expression

$$F_{\text{vib}}(V,T) = k_B T \int_0^{\infty} \left\{ \ln \left[2 \sinh \left(\frac{h\upsilon}{2k_B T} \right) \right] g(\upsilon) \right\} d\upsilon, \tag{2}$$

where k_B is Boltzmann's constant, and h is Plank's constant. A review by van de Walle and Ceder[19] is recommended for further reading on the quasi-harmonic theory within the framework of alloy thermodynamics. The 0K elastic constants for each phase are calculated using the method described in a previous work[20]

Discussion

Free energy surfaces and thermodynamics

The free energy surfaces for both the austenite and martensite phases are plotted together in Figure 1. For temperatures up to 400 K, we see that the martensite phase has the lowest energy at each reduced volume. Furthermore, the surfaces do not intersect at any point, indicating that one phase remains energetically favorable at all temperatures. This is consistent with the experimental observation that stoichiometric Ni_2MnIn does not undergo a martensitic transition upon cooling

Other thermodynamic properties for each phase are obtained from the free energy; namely entropy is defined as

$$S = \frac{\partial F(T)}{\partial T}, \tag{3}$$

and specific heat is given as

$$C_P = T \frac{\partial S}{\partial T}. \tag{4}$$

These are plotted for each volume in Figure 2. We see that the entropy is lowest for the austenite structure at all temperatures. This suggests that the tetragonal structure will be most stable at room temperature and will remain favorable over the cubic structure as temperature is lowered. No intersection of the entropy curves again indicates that no phase transformation will occur. However, this result contradicts the observation that cubic $L2_1$ is the most stable structure at room temperature. This suggests that other contributions to the free energy (i.e. electronic or anharmonic) may play a role in stabilizing the austenite phase. Certainly more calculations, to include explicit treatment of magnetic degrees of freedom, are needed.

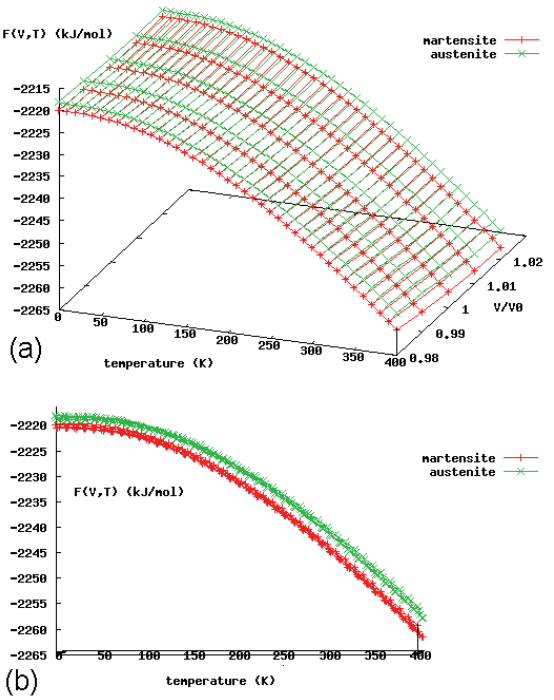

Figure 1: (a) Free energy surface as a function of temperature and reduced volume for both the austenite and martensite phases of Ni2MnIn. Energies were calculated according to Equation (1). (b) Projection of each energy surface onto the F(V,T)-T plane.

The title of the paper should be in bold, Times 14 point size at the top of the document as illustrated. This should be followed by all the authors' names. Affiliations of the authors should be presented as footnotes. Footnotes should be numbered consecutively in arabic numbers. The index of the footnotes, in superscript, should be placed in the upper-right corner of the word that is to be annotated. Here is an example. The title, and the authors' names, should be centered in the document.

Elastic Constants

TThe 0K elastic constants of the cubic austenite and tetragonal martensite of Ni_2MnIn are listed in Table I. The bulk modulus of each phase is found by fitting the curve of total energy vs. volume to the third-order Birch–Murnaghan equation of state. The previously calculated values for the Ni_2MnGa system are also included for comparison.

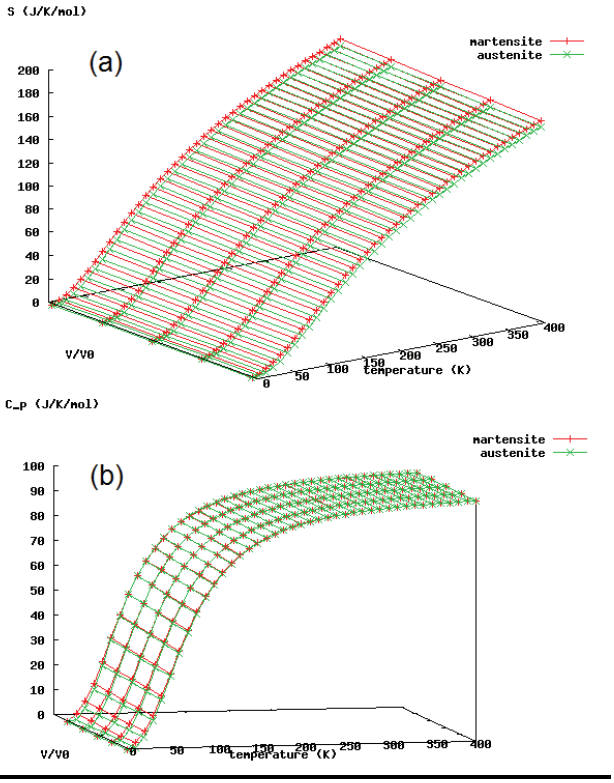

Figure 2: Values of (a) entropy and (b) specific heat calculated from the total free energy surfaces in Figure 1.

Table 1: Elastic moduli calculated for each phase. All values are reported in GPa.

	austenite phase					martensite phase							
	B	$C\prime$	C_{11}	C_{12}	C_{44}	B	$C\prime$	C_{11}	C_{12}	C_{13}	C_{33}	C_{44}	C_{66}
Ni_2MnIn	133	32.9	208	142	21.4	132	85.5	219	47.5	129	140	105	12.7
Ni_2MnGa[20]	155	6.1	163	151	110	155.6	89	249	71	141	193	101	56

Conclusions

We have used the quasi-harmonic approximation of lattice theory to evaluate the phase stability of stoichiometric Ni_2MnIn. We have considered two possible structures: cubic and tetragonal with $c/a \approx 1.41$. From the calculated free energy surfaces, we evaluated the entropy of each phase, finding theoretical contradiction to the stability of $L2_1$ Ni_2MnIn. Future work will focus on similar calculations for other phases of the Ni-Mn-In alloy system, namely an alternative $L1_0$ structure (tetragonal with $c/a < 1$) and modulated phases. Attention will be given to magnetic degrees of freedom in an attempt to find better agreement with experiment.

Acknowledgement

The research reported here is funded in part by NSF-IMI. K. Williams acknowledges support from the National Science Foundation through its Integrative Education and Research Traineeship program.

References

1. S. J. Murray, M. Marioni, S. M. Allen, R. C. O'Handley and T. A. Lograsso, Applied Physics Letters **77** (6), 886-888 (2000).
2. T. Krenke, E. Duman, M. Acet, E. F. Wassermann, X. Moya, L. Manosa, A. Planes, E. Suard and B. Ouladdiaf, Physical Review B (Condensed Matter and Materials Physics) **75** (10), 104414-104416 (2007).
3. Y. Sutou, Y. Imano, N. Koeda, T. Omori, R. Kainuma, K. Ishida and K. Oikawa, Applied Physics Letters **85** (19), 4358-4360 (2004).
4. Z. D. Han, D. H. Wang, C. L. Zhang, S. L. Tang, B. X. Gu and Y. W. Du, Applied Physics Letters **89** (18), 182507-182503 (2006).
5. V. K. Sharma, M. K. Chattopadhyay and S. B. Roy, Journal of Physics D: Applied Physics **40** (7), 1869-1873 (2007).
6. I. Dubenko, M. Khan, A. K. Pathak, B. R. Gautam, S. Stadler and N. Ali, Journal of Magnetism and Magnetic Materials **321** (7), 754-757 (2009).
7. S. Y. Yu, Z. H. Liu, G. D. Liu, J. L. Chen, Z. X. Cao, G. H. Wu, B. Zhang and X. X. Zhang, Applied Physics Letters **89** (16), 162503-162503 (2006).
8. V. K. Sharma, M. K. Chattopadhyay, K. H. B. Shaeb, A. Chouhan and S. B. Roy, Applied Physics Letters **89** (22), 222509-222503 (2006).
9. V. K. Sharma, M. K. Chattopadhyay and S. B. Roy, Physical Review B (Condensed Matter and Materials Physics) **76** (14), 140401-140404 (2007).
10. R. Y. Umetsu, W. Ito, K. Ito, K. Koyama, A. Fujita, K. Oikawa, T. Kanomata, R. Kainuma and K. Ishida, Scripta Materialia **60** (1), 25-28 (2009).
11. J. H. Van Vleck, Reviews of Modern Physics **34** (4), 681 (1962).
12. V. V. Godlevsky and K. M. Rabe, Physical Review B **63** (13), 134407 (2001).
13. A. T. Zayak, P. Entel, K. M. Rabe, W. A. Adeagbo and M. Acet, Physical Review B **72** (5), 054113 (2005).
14. J. Enkovaara, A. Ayuela, L. Nordstrom and R. M. Nieminen, Journal of Applied Physics **91** (10), 7798-7800 (2002).
15. M. A. Uijttewaal, T. Hickel, J. Neugebauer, M. E. Gruner and P. Entel, Physical Review Letters **102** (3), 035702-035704 (2009).

16. G. Kresse and J. Furthmller, Physical Review B **54** (Copyright (C) 2009 The American Physical Society), 11169 (1996).
17. P. E. Blochl, Physical Review B **50** (Copyright (C) 2009 The American Physical Society), 17953 (1994).
18. J. P. Perdew, K. Burke and M. Ernzerhof, Physical Review Letters **77** (Copyright (C) 2009 The American Physical Society), 3865 (1996).
19. A. van de Walle and G. Ceder, Reviews of Modern Physics **74** (Copyright (C) 2009 The American Physical Society), 11 (2002).
20. S. O. Kart, M. Uludogan, I. Karaman and T. Cagin, physica status solidi (a) **205** (5), 1026-1035 (2008).